

W. W. Yuen

Department of Mechanical and
Environmental Engineering,
University of California,
Santa Barbara, Calif. 93106

A Simplified Approach to the Evaluation of the Geometric-Mean Transmittance and Absorptance for Gas Enclosures

Utilizing a simple mathematical relation and Stoke's theorem, the geometric-mean transmittance and total absorptance between an infinitesimal area and a finite planar element is reduced to a line integral around the planar element and an area integral. A concept of fundamental solutions is introduced. These are solutions in which the finite areas are horizontal right triangle with three specific orientations. Based on superposition, solutions for arbitrary finite areas are shown to be readily generated algebraically from these fundamental solutions. The geometric-mean transmittance and total absorptance between two finite areas are reduced to single numerical integrations, thus reducing much of the mathematical complexity.

Fundamental solutions for mean beam lengths of the geometric-mean total absorptance in the weak-band, strong-band and very-strong-band limits are generated analytically in closed form. Based on the existing one-dimensional wide band correlation, these limiting expressions are shown to be sufficient for the calculation of the geometric-mean total absorptance at all optical thicknesses. A sample calculation is presented.

Introduction

In many heat transfer calculations for practical engineering systems with high temperature such as fires and combustion furnaces, the evaluation of the surface-surface and surface-medium radiative exchange in an enclosure with an intervening absorbing-emitting medium is a problem of considerable importance. Mathematically, this task involves the evaluation of the so-called geometric-mean transmittance and absorptance for the considered enclosure.

Formally, definitions of the geometric-mean transmittance and absorptance are quite simple and straight-forward and their importance was realized more than 30 years ago [1]. A great deal of effort has been made since then to tabulate these quantities for various systems. The success of these efforts, however, is quite limited largely because of the mathematical complexity of the problem. Today, exact evaluations for these quantities are restricted only to a few cases with special geometric symmetry or optical thickness limits [2-6]. For most other cases, the current state-of-the-art technique is to utilize an empirical "mean beam length" and the corresponding one-dimensional results [1, 2]. While this method appears to be reasonably accurate for some selected enclosures, its applicability to general enclosures still remains unproven and has uncertain accuracy.

The major difficulty in the calculation of the geometric-mean transmittance and absorptance for a given enclosure is that they require the evaluation of a complicated integral. The integral involves not only the geometry of the two considered surfaces, but also their relative orientation. Because of the presence of angular variables, many traditional numerical techniques for integral evaluation cannot be applied. The integral can also become singular for some selected cases. The objective of this work is to show that by using a simple mathematical relation and Stoke's theorem, the geometric-mean transmittance and absorptance between an infinitesimal area element and a finite area can be expressed as sums of a simple line integral around the boundary of the finite surface and an area integral. These integrals can be evaluated analytically for some selected cases. For all cases, they can be tabulated numerically by standard technique.

For general application, the present work proposes a concept of fundamental solutions. These solutions are geometric-mean transmittance and absorptance between an infinitesimal area of arbitrary orientation and horizontal right triangles of three specific orientations. Utilizing the principle of superposition, the geometric-mean transmittance and absorptance between an infinitesimal area and any finite area can be written as sums and differences of these fundamental solutions. Based on the present approach, these fundamental solutions are readily generated in closed-form. If the intervening medium is a non-gray gas, the important physical quantity is the geometric-mean total absorptance (which is the integral over wavelengths of the geometric-mean absorptance). Fundamental solutions for this quantity in the weak-band, strong-band and very-strong-band limits are also readily generated. Using the existing wide-band correlations, these limiting expressions are demonstrated to be sufficient for the evaluation of the geometric-mean total absorptance at all optical thickness. It is interesting to note that until now, only tabulations of the weak-band limit of the geometric-mean total absorptance for some selected simple systems are available in the literature [1, 2, 4] largely because of the mathematical complexity.

To illustrate the accuracy and the simplicity of the present approach, the weak-band, strong-band and very-strong-band limit of the total geometric-mean absorptance between two rectangles of different orientations is generated. For the weak-band cases which were considered by Dunkle [4] with a different approach, the agreement is excellent. The present approach, however, is readily seen to be more general and simple to use.

Mathematical Formulation

Utilizing the geometry and coordinate system as shown in Fig. 1, the geometric-mean transmittance between areas dA_1 and A_2 , $\tau_{\lambda,d1-2}$, can be written

$$\tau_{\lambda,d1-2} = \frac{1}{F_{d1-2}} \int_{A_2} \frac{(\mathbf{n}_1 \cdot \mathbf{r}_1)(\mathbf{n}_2 \cdot \mathbf{r}_2)e^{-a_\lambda r}}{\pi r^2} dA_2 \quad (1)$$

where F_{d1-2} is the shape factor [1] between dA_1 and A_2 , \mathbf{n}_1 and \mathbf{n}_2 are the unit normal vectors to areas dA_1 and dA_2 respectively, \mathbf{r}_1 is a unit vector pointing away from dA_1 to dA_2 , r is the distance between the two areas, and a_λ is the absorption coefficient. Physically, $\tau_{\lambda,d1-2}$ is the fraction of energy leaving surface dA_1 which is transmitted

Contributed by the Heat Transfer Division for publication in the JOURNAL OF HEAT TRANSFER. Manuscript received by the Heat Transfer Division December 8, 1980.

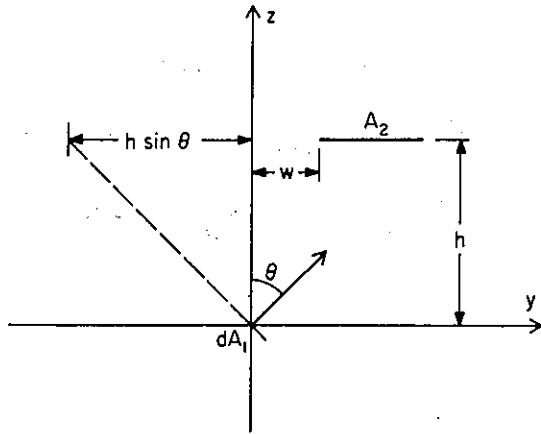


Fig. 1 Coordinate system used in equation (1)

through the medium and arrives at A_2 . To calculate the fraction of energy leaving surface dA_1 which is absorbed by the intervening medium, the concept of geometric-mean absorptance is important. It is

$$\alpha_{\lambda,d1-2} = \frac{1}{F_{d1-2}} \int_{A_2} \frac{(\mathbf{n}_1 \cdot \mathbf{r}_1)(\mathbf{n}_2 \cdot \mathbf{r}_1)(1 - e^{-\alpha_\lambda r})}{\pi r^2} dA_2 \quad (2)$$

If the medium is a non-gray gas with absorption bands, equation (2) can be integrated over one band to yield the total geometric mean absorptance as

$$\alpha_{i,d1-2} = \int_{\Delta_i} \alpha_{\lambda,d1-2} d\lambda = \frac{1}{F_{d1-2}} \int_{A_2} \frac{(\mathbf{n}_1 \cdot \mathbf{r}_1)(\mathbf{n}_2 \cdot \mathbf{r}_1) \bar{A}_i(r)}{\pi r^2} dA_2 \quad (3)$$

where $\int_{\Delta_i} d\lambda$ represents integration over the i th absorption band and \bar{A}_i is the corresponding effective bandwidth for a one-dimensional system of thickness r . Effective bandwidths for various important bands for different gases have been demonstrated to be adequately approximated by the so-called wide-band correlation [2]. The correlation proposed by Edwards, et al. [2, 7] is presented in Table 1.

Substituting results presented in Table 1 into equation (3), it can be readily seen that the evaluation of $\alpha_{i,d1-2}$ requires only the following integrals:

$$R_{d1-2} = \frac{1}{F_{d1-2}} \int_{A_2} \frac{(\mathbf{n}_1 \cdot \mathbf{r}_1)(\mathbf{n}_2 \cdot \mathbf{r}_2)}{\pi r} dA_2 \quad (4)$$

$$(S_{d1-2})^{1/2} = \frac{1}{F_{d1-2}} \int_{A_2} \frac{(\mathbf{n}_1 \cdot \mathbf{r}_1)(\mathbf{n}_2 \cdot \mathbf{r}_1)}{\pi r^{3/2}} dA_2 \quad (5)$$

$$\ln W_{d1-2} = \frac{1}{F_{d1-2}} \int_{A_2} \frac{(\mathbf{n}_1 \cdot \mathbf{r}_1)(\mathbf{n}_2 \cdot \mathbf{r}_1)}{\pi r^2} \ln r dA_2 \quad (6)$$

It is interesting to note that R_{d1-2} is the weak-band geometric mean beam length originally introduced by Dunkle [4]. Since $\bar{A}_i(r)$ is proportional to $r^{1/2}$ and $\ln r$ in the strong band and very-strong band limit, respectively. S_{d1-2} and W_{d1-2} can be interpreted as the corresponding geometric mean beam length in those limits. For two finite areas A_1 and A_2 , equations (4, 5) and (6) are generalized to

$$R_{1-2} = \frac{1}{A_1 F_{12}} \int_{A_1} F_{d1-2} R_{d1-2} dA_1, \quad (4a)$$

$$S_{1-2}^{1/2} = \frac{1}{A_1 F_{12}} \int_{A_1} F_{d1-2} S_{d1-2}^{1/2} dA_1, \quad (5a)$$

$$\ln W_{1-2} = \frac{1}{A_1 F_{12}} \int_{A_1} F_{d1-2} \ln W_{d1-2} dA_1. \quad (6a)$$

In terms of R_{1-2} , S_{1-2} and W_{1-2} , a correlation analogous to Table 1 for the total geometric-mean absorptance between two finite areas A_1 and A_2 can be generated. It is presented in Table 2.

Since equations (1, 4, 5), and (6) are all of the same general form as the left hand side of equation (A3) in Appendix I, they can be simplified. Equation (1), for example, can be written as

$$\pi F_{d1-2} \tau_{\lambda,d1-2} = \int_{S_2} g_1(r) (\mathbf{r}_1 \times \mathbf{n}_1) \cdot d\mathbf{S}_2 + \int_{A_2} (\mathbf{n}_1 \cdot \mathbf{n}_2) \left[g'_1(r) + \frac{g_1(r)}{r} \right] dA_2 \quad (7)$$

where $g_1(r)$ satisfies the equation

$$g'_1(r) - \frac{g_1(r)}{r} = \frac{e^{-\alpha_\lambda r}}{r^2} \quad (8)$$

Equations (4, 5), and (6) can be written as

$$\pi F_{d1-2} R_{d1-2} = \int_{S_2} g_2(r) (\mathbf{r}_1 \times \mathbf{n}_1) \cdot d\mathbf{S}_2 + \int_{A_2} (\mathbf{n}_1 \cdot \mathbf{n}_2) \left[g'_2(r) + \frac{g_2(r)}{r} \right] dA_2 \quad (9)$$

$$\pi F_{d1-2} S_{d1-2}^{1/2} = \int_{S_2} g_3(r) (\mathbf{r}_1 \times \mathbf{n}_1) \cdot d\mathbf{S}_2 + \int_{A_2} (\mathbf{n}_1 \cdot \mathbf{n}_2) \left[g'_3(r) + \frac{g_3(r)}{r} \right] dA_2 \quad (10)$$

$$\pi F_{d1-2} \ln W_{d1-2} = \int_{S_2} g_4(r) (\mathbf{r}_1 \times \mathbf{n}_1) \cdot d\mathbf{S}_2 + \int_{A_2} (\mathbf{n}_1 \cdot \mathbf{n}_2) \left[g'_4(r) + \frac{g_4(r)}{r} \right] dA_2 \quad (11)$$

with $g_2(r)$, $g_3(r)$, and $g_4(r)$ satisfying

Nomenclature

α_λ = absorption coefficient

A_1, A_2 = area elements

\bar{A}_i = effective bandwidth of the i th band

d = parameter defined in Fig. 2(b)

E_3 = exponential function

$F\left(\Gamma, \frac{1}{2^{1/2}}\right)$ = elliptic function of the first kind

f_{i-j} = shape factor between area A_i and A_j

g_i ($i = 1, 2, 3, 4$) = functions defined by equations (15) thru (18)

G = functions defined by equations (22, 26) and (30)

h = parameter defined in Fig. 2(a)

H = functions defined by equations (23, 28) and (31)

$\mathbf{n}_1, \mathbf{n}_2$ = unit vectors defined in Fig. 1

$\mathbf{r}_1, \mathbf{r}_2$ = unit vectors defined by equations (1) and (2)

r = distance between areas dA_1 and dA_2

R_{i-j} = weak-band geometric mean beam length, equation (4)

S_{i-j} = strong-band geometric mean beam length, equation (4)

u = parameter defined in Fig. 2(b)

v = parameter defined in Fig. 2(b)

w = parameter defined in Fig. 2(b)

W_{1-2} = very-strong-band geometric mean

beam length, equation (6)

Z_I, Z_{II}, Z_{III} = fundamental solutions defined by equations (21, 32) and (33)

Z_{i-j} = generalized mean beam length defined by equation (21)

$\alpha_{\lambda,1-2}$ = geometric-mean absorptance defined by equation (2)

$\alpha_{i,1-2}$ = total geometric-mean absorptance of the i th band

$\gamma(y)$ = function defined by equation (29)

θ = parameter defined in Fig. 2(a)

λ = wavelength

$\rho(x)$ = function defined by equation (27)

$\tau_{\lambda,1-2}$ = geometric-mean transmittance defined by equation (1)

Table 1 Effective bandwidth correlation equations for isothermal gas

Pressure-broadening Parameter $\beta = \frac{C_2^2 P_e}{4C_1 C_3}$	Lower limit of \bar{A} η, cm^{-1}	Upper limit of \bar{A} η, cm^{-1}	Effective bandwidth \bar{A} η, cm^{-1}
$\beta \leq 1$	0	βC_3	$\bar{A} = C_1 X$
	βC_3	$C_3(2 - \beta)$	$\bar{A} = C_2(X P_e)^{1/2} - \beta C_3$
	$C_3(2 - \beta)$	∞	$\bar{A} = C_3 \left(\ln \frac{C_2^2 X P_e}{4C_3^2} + 2 - \beta \right)$
$\beta > 1$	0	C_3	$\bar{A} = C_1 X$
	C_3	∞	$\bar{A} = C_3 \left(\ln \frac{C_1 X}{C_3} + 1 \right)$

$C_1, C_2, C_3, b,$ and n given in reference [7]. X is mass path length, $\rho S, \text{g/m}^2$. $P_e = [(P + P_{N_2})/P_0]^n$ where $P_{N_2} = 1 \text{ atm}$, P is partial pressure of absorbing gas, and P_{N_2} is partial pressure of N_2 broadening gas in atmospheres.

Table 2 Effective bandwidth correlation equations for multidimensional isothermal gas

Pressure-broadening Parameter $\beta = \frac{C_2^2 P_e}{4C_1 C_3}$	Lower limit of \bar{A} η, cm^{-1}	Upper limit of \bar{A} η, cm^{-1}	Effective bandwidth \bar{A} η, cm^{-1}
$\beta \leq 1$	0	βC_3	$\bar{A} = C_1 \rho R_{1-2}$
	βC_3	$C_3(2 - \beta)$	$\bar{A} = C_2(\rho S_{1-2} P_e)^{1/2} - \beta C_3$
	$C_3(2 - \beta)$	∞	$\bar{A} = C_3 \left(\ln \frac{C_2^2 \rho W_{1-2} P_e}{4C_3^2} + 2 - \beta \right)$
$\beta > 1$	0	C_3	$\bar{A} = C_1 \rho R_{1-2}$
	C_3	∞	$\bar{A} = C_3 \left(\ln \frac{C_1 \rho W_{1-2}}{C_3} + 1 \right)$

$C_1, C_2, C_3, b,$ and n given in reference [7]. ρ is mass density g/m^3 , and S is pathlength m , $P_e = [(P + P_{N_2})/P_0]^n$ where $P_{N_2} = 1 \text{ atm}$, P is partial pressure of absorbing gas, and P_{N_2} is partial pressure of N_2 broadening gas in atmospheres.

$$g'_2(r) - \frac{g_2(r)}{r} = \frac{1}{r} \quad (12)$$

$$g'_3(r) - \frac{g_3(r)}{r} = \frac{1}{r^{3/2}} \quad (13)$$

$$g'_4(r) - \frac{g_4(r)}{r} = \frac{\ln r}{r^2} \quad (14)$$

Equations (8, 12, 13), and (14) can be readily solved to yield

$$g_1(r) = -\frac{E_3(a_\lambda r)}{r} \quad (15)$$

$$g_2(r) = -1 \quad (16)$$

$$g_3(r) = -\frac{2}{3r^{1/2}} \quad (17)$$

$$g_4(r) = -\frac{\ln r}{2r} - \frac{1}{4r} \quad (18)$$

with $E_3(a_\lambda r)$ in equation (15) being the familiar exponential integral function defined by

$$E_n(x) = \int_1^\infty \frac{e^{-xt}}{t^n} dt, \quad n \geq 1 \quad (19)$$

Utilizing equations (15-18), equations (7, 9, 10), and (11) become

$$\pi F_{d1-2} r_{\lambda, d1-2} = - \int_{S_2} \frac{E_3(a_\lambda r)}{r} (\mathbf{r}_1 \times \mathbf{n}_1) \cdot d\mathbf{S}_2 + \int_{A_2} (\mathbf{n}_1 \cdot \mathbf{n}_2) \frac{a_\lambda}{r} E_2(a_\lambda r) dA_2 \quad (20)$$

$$\pi F_{d1-2} R_{d1-2} = - \int_{S_2} (\mathbf{r}_1 \times \mathbf{n}_1) \cdot d\mathbf{S}_2 - \int_{A_2} (\mathbf{n}_1 \cdot \mathbf{n}_2) \frac{dA_2}{r} \quad (21)$$

$$\pi F_{d1-2} S_{d1-2}^{1/2} = -\frac{2}{3} \int_{S_2} \frac{(\mathbf{r}_1 \times \mathbf{n}_1) \cdot d\mathbf{S}_2}{r^{1/2}} - \frac{1}{3} \int_{A_2} \frac{(\mathbf{n}_1 \cdot \mathbf{n}_2) dA_2}{r^{3/2}} \quad (22)$$

$$\pi F_{d1-2} \ln W_{d1-2} = -\frac{1}{2} \int_{S_2} \left(\frac{\ln r}{r} + \frac{1}{2r} \right) (\mathbf{r}_1 \times \mathbf{n}_1) \cdot d\mathbf{S}_2 - \frac{1}{2} \int_{A_2} (\mathbf{n}_1 \cdot \mathbf{n}_2) \frac{dA_2}{r^2} \quad (23)$$

In terms of actual evaluation, equations (20-23) represent a great reduction in complexity in contrast to equations (1, 4, 5), and (6).

Fundamental Solutions

Equations (20-23) can be readily evaluated in closed-form for some systems with simple geometry. But for general application, the most important results are fundamental solutions for these expressions in which dA_1 is an infinitesimal area at the origin with arbitrary orientation and A_2 is a right triangle at a horizontal plane above the origin. It can be shown that it is sufficient to consider only four particular orientations of A_2 . The geometry and the associated coordinate systems for the four fundamental solutions are illustrated in Figs. 2(a) and 2(b). The superposition procedure can be generated from these fundamental solutions as outlined in Appendix II.

For the right triangle I as shown in Fig. 2(b), equations (20-22) and (23) can be readily simplified into the following form

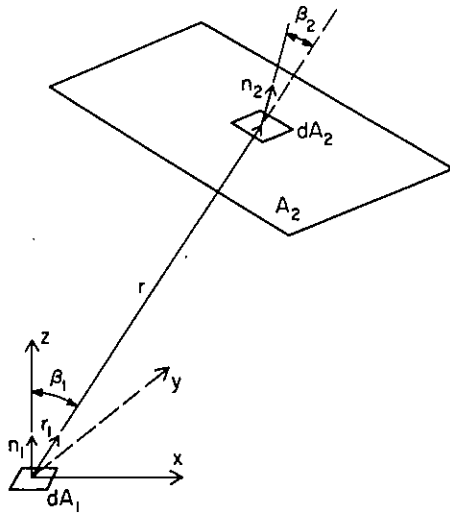


Fig. 2(a) Side-view of the relative position and orientation of dA_1 and A_2 for the fundamental solutions

$$Z_1(u, v, w, h, \theta) = (h \sin \theta - w \cos \theta)G(0, u, 1, 0, w^2 + h^2) \\ + u \cos \theta G(w, w + v, 1, 0, u^2 + h^2) \\ + (w \cos \theta - h \sin \theta)G\left(0, u, \frac{u^2 + v^2 + 2wv}{u^2}, \frac{2wv}{u}, w^2 + h^2\right) \\ - \cos \theta H(u, v, w, 0, 0). \quad (24)$$

For the geometric-mean transmittance, Z_1 stands for $(F_{d1-2} \tau_{\lambda, d1-2})^I$, and $G(m, n, A, B, C)$ and $H(u, v, w, d, \phi)$ are given by

$$G(m, n, A, B, C) = \frac{1}{\pi} \int_m^n \frac{E_3[a_\lambda (At^2 + Bt + C)^{1/2}]}{(At^2 + Bt + C)} dt \quad (25)$$

$$H(u, v, w, d, \phi) = -\frac{a_\lambda}{\pi} \int_{x_1}^{x_2} \int_{y_1}^{y_2} \frac{E_2[a_\lambda (x^2 + y^2 + h^2)^{1/2}]}{(x^2 + y^2 + h^2)^{1/2}} dy dx \quad (26)$$

where $y_1 = w \cos \phi$, $y_2 = w \cos \phi + v/u(x - d - w \sin \phi)$, $x_1 = w \sin \phi + d$ and $x_2 = w \sin \phi + d + u$. For the weak-band limit of the geometric-mean total absorptance, Z_1 stands for $(F_{d1-2} R_{d1-2})^I$ with

$$G(m, n, A, B, C) = \frac{1}{\pi A^{1/2}} \ln \left[\frac{2(An^2 + Bn + C)^{1/2} + 2A^{1/2}n + A^{1/2}B}{2(Am^2 + Bm + C)^{1/2} + 2A^{1/2}m + A^{1/2}B} \right] \quad (27)$$

$$H(u, v, w, d, \phi) = \frac{1}{\pi} \int_{x_1}^{x_2} \ln \left[\frac{(y_2^2 + x^2 + h^2)^{1/2} + y_2}{(y_1^2 + x^2 + h^2)^{1/2} + y_1} \right] dx. \quad (28)$$

Equation (28) can be integrated in closed-form with a standard integration table [8]. For the strong-band limit of the geometric-mean total absorptance, Z_1 stands for $(F_{d1-2} S_{d1-2}^{1/2})^I$ with

$$G(m, n, A, B, C) = \frac{4}{3\pi[A(4AC - B^2)]^{1/4}} \left[\frac{n + B/2A}{|n + B/2A|} F\left(\rho(n), \frac{1}{2^{1/2}}\right) - \frac{m + B/2A}{|m + B/2A|} F\left(\rho(m), \frac{1}{2^{1/2}}\right) \right] \quad (29)$$

where

$$\rho(x) = \cos^{-1} \left[\frac{1}{\frac{(2Ax + B)^2}{4AC - B^2} + 1} \right]^{1/4} \quad (30)$$

The function $F(\Gamma, 1/2^{1/2})$ in equation (29) is the elliptic integral of the first kind. The function $H(u, v, w, d)$ is given by

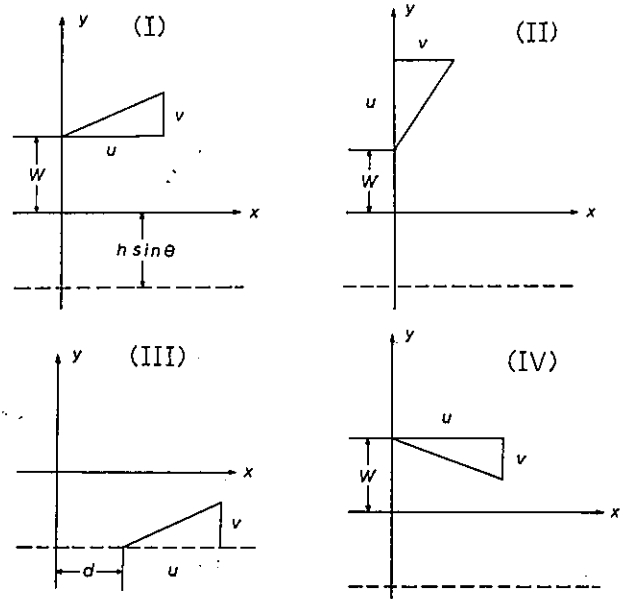


Fig. 2(b) Top view of orientations of A_2 for the four fundamental solutions

$$H(u, v, w, d, \phi) = \frac{2^{1/2}}{3} \int_{x_1}^{x_2} \frac{1}{(x^2 + h^2)^{1/4}} \left[F\left(\gamma(y_2), \frac{1}{2^{1/2}}\right) - F\left(\gamma(y_1), \frac{1}{2^{1/2}}\right) \right] dx \quad (31)$$

where

$$\gamma(y) = \cos^{-1} \left[\frac{x^2 + h^2}{y^2 + x^2 + h^2} \right]^{1/4} \quad (32)$$

At the very-strong-band limit, Z_1 stands for $(F_{d1-2} \ln w_{d1-2})^I$ where

$$G(m, n, A, B, C) = \frac{1}{4\pi} \int_m^n \frac{\ln [At^2 + Bt + C]}{[At^2 + Bt + C]} dt \\ + \frac{1}{2\pi(4AC - B^2)^{1/2}} \left[\tan^{-1} \frac{B + 2An}{(4AC - B^2)^{1/2}} - \tan^{-1} \frac{B + 2Am}{(4AC - B^2)^{1/2}} \right] \quad (33)$$

and

$$H(u, v, w, d, \phi) = \frac{1}{2\pi} \int_{x_1}^{x_2} \frac{1}{(x^2 + h^2)^{1/2}} \left[\tan^{-1} \frac{y_2}{(x^2 + h^2)^{1/2}} - \tan^{-1} \frac{y_1}{(x^2 + h^2)^{1/2}} \right] dx \quad (34)$$

Similarly, the fundamental solutions for right triangles II, III, and IV as shown in Fig. 2(b) are given by

$$Z_{II}(u, v, w, h, \theta) = -[(u + w) \cos \theta - h \sin \theta] G\left(0, v, 1, 0, h^2 + (u + w)^2\right) \\ + \frac{v}{u} (w \cos \theta - h \sin \theta) G\left(w, w + u, \frac{u^2 + v^2}{u^2}, -\frac{2v^2}{u^2} w, \frac{w^2 v^2}{u^2} + h^2\right) - \cos \theta H(u, v, w, 0, \pi/2) \quad (35)$$

$$Z_{III}(u, v, d, h, \theta) = -h \sin \theta (\cos \theta + 1) G(d, d + u, 1, 0, h^2(1 + \sin^2 \theta)) \\ - (u + d) \cos \theta G(-h \sin \theta, -h \sin \theta + v, 1, 0, h^2 + (u + d)^2) \\ + \left[h \sin \theta (1 + \cos \theta) + \frac{v}{u} d \cos \theta \right] G\left(d, d + u, \frac{u^2 + v^2}{u^2}, 2 \frac{v}{u} \left(-h \sin \theta - \frac{v}{u} d\right), h^2 + \left(h \sin \theta + \frac{v}{u} d\right)^2\right) \\ - \cos \theta H(u, v, -h \sin \theta, d, 0) \quad (36)$$

$$Z_{IV}(u, v, d, h, \theta) = (w \cos \theta - h \sin \theta) G(0, u, 1, 0, w^2 + h^2) - u \cos \theta G(w, w - v, 1, 0, u^2 + h^2) + (h \sin \theta - w \cos \theta) G(0, u, 1, + u^2/u^2, -2wv/u, w^2 + h^2) + \cos \theta H(u, -v, w, 0, 0) \quad (36a)$$

The functions G and H in equations (35) and (36) are defined identically as in equations (25-35).

To demonstrate the utility and simplicity of the present mathematical approach in application for finite area, the weak-band, strong-band, and very-strong-band limits of the geometric-mean beam length between two rectangular plates with orientation as shown in Fig. 3 is now calculated. This example is selected because some results in the weak-band limit with $\beta = 0$ and $\beta = \pi/2$ have already been tabulated by Dunkle [4] with a different approach. A direct comparison is thus possible. The strong-band and very-strong-band limits, on the other hand, have never been reported in the literature.

Consider a differential area dA_I at $(x, y, 0)$; A_{II} can be readily broken up relative to dA_I into four fundamental right triangles. Using superposition, the three limits of the geometric mean beam can be written in the following generalized form

$$Z_{dA_I-A_{II}} = \sum_{i=1}^4 Z_{dA_I-A_i} \quad (37)$$

where

$$Z_{dA_I-A_1} = Z_I \left(\frac{a}{2} - y, b, -x \cos \beta, h + x \sin \beta, \beta \right) \quad (38)$$

$$Z_{dA_I-A_2} = Z_{II} \left(b, \frac{a}{2} - y, -x \cos \beta, h + x \sin \beta, \beta \right) \quad (39)$$

$$Z_{dA_I-A_3} = Z_{II} \left(b, y + \frac{a}{2}, -x \cos \beta, h + x \sin \beta, \beta \right) \quad (40)$$

$$Z_{dA_I-A_4} = Z_I \left(y + \frac{a}{2}, b, -x \cos \beta, h + x \sin \beta, \beta \right) \quad (41)$$

Equation (37) can be integrated over A_I to yield

$$Z_{A_I-A_{II}} = \frac{2}{ab} \int_0^a \int_0^b Z_{dA_I-A_{II}} dx dy \quad (42)$$

In the above expression, $Z_{A_I-A_{II}}$ stands for $F_{A_I-A_{II}} R_{A_I-A_{II}}$, $F_{A_I-A_{II}} S_{A_I-A_{II}}^{1/2}$ and $F_{A_I-A_{II}} \ln W_{A_I-A_{II}}$ in the weak-band, strong-band and very-strong-band limit, respectively.

Equation (42) can be readily evaluated numerically in all three limits. For all cases, the integral converges quickly with no difficulty. Results for the three limits for various values of a , b , and β with $h = 1.0$ are presented in Tables 3, 4 and 5. For the weak-band cases with $\beta = 0$ and $\beta = \pi/2$, the agreement with Dunkle's result [4] is exact. It is interesting to note that for the considered cases, the difference between the geometric-mean beam lengths at the three limits is quite insignificant.

Acknowledgment

This work is based partially upon work supported by the National Science Foundation Grant No. ENG78-05587.

APPENDIX I

For an arbitrary function $f(r)$ and utilizing the coordinate system as shown in Fig. 1, it can be shown by direct differentiations that the following identity holds.

$$\nabla \times [f(r) \mathbf{r}_1 \times \mathbf{n}_1]$$

$$= (\mathbf{n}_1 \cdot \mathbf{r}_1) \mathbf{r}_1 \left[f'(r) - \frac{f(r)}{r} \right] - \mathbf{n}_1 \left[f'(r) + \frac{f(r)}{r} \right] \quad (A1)$$

In the above expression, ∇ is the gradient operator, \mathbf{n}_1 and \mathbf{r}_1 are vectors as defined in Fig. 1 and $f'(r) = df/dr$. If equation (A1) is integrated over the area A_2 , one obtains

Table 3 $F_{A_I-A_{II}} R_{A_I-A_{II}}$ between two rectangular plates with different values of a , b , and β with $h = 1.0$. (Values in parentheses are $R_{A_I-A_{II}}$).

β	$a \backslash b$	0.4	1.0	4.0
$\pi/2$	0.4	(1.20)	(1.47)	(2.84)
		0.006	0.022	0.054
	1.0	(1.25)	(1.55)	(3.02)
		0.015	0.051	0.133
4.0	(1.43)	(1.76)	(3.40)	
	0.030	0.120	0.415	
$\pi/4$	0.4	(1.14)	(1.35)	(2.28)
		0.032	0.066	0.123
	1.0	(1.19)	(1.39)	(2.34)
		0.070	0.150	0.295
4.0	(1.33)	(1.56)	(2.65)	
	0.141	0.329	0.838	
0	0.4	(1.02)	(1.06)	(1.20)
		0.047	0.102	0.194
	1.0	(1.06)	(1.11)	(1.25)
		0.102	0.222	0.431
4.0	(1.20)	(1.25)	(1.42)	
	0.194	0.431	0.897	

Table 4 $F_{A_I-A_{II}} S_{A_I-A_{II}}^{1/2}$ between two rectangular plates with different values of a , b , and β with $h = 1.0$. (values in parentheses are $S_{A_I-A_{II}}$).

β	$a \backslash b$	0.4	1.0	4.0
$\pi/2$	0.4	(1.00)	(1.44)	(2.66)
		0.005	0.018	0.031
	1.0	(1.17)	(1.54)	(2.91)
		0.013	0.041	0.075
4.0	(1.41)	(1.75)	(3.25)	
	0.025	0.090	0.220	
$\pi/4$	0.4	(1.00)	(1.35)	(2.19)
		0.028	0.057	0.080
	1.0	(1.18)	(1.38)	(2.25)
		0.064	0.127	0.189
4.0	(1.30)	(1.53)	(2.57)	
	0.121	0.261	0.507	
0	0.4	(1.04)	(1.06)	(1.19)
		0.047	0.099	0.177
	1.0	(1.09)	(1.11)	(1.26)
		0.099	0.211	0.384
4.0	(1.18)	(1.23)	(1.45)	
	0.176	0.384	0.746	

Table 5 $F_{A_I-A_{II}} \ln W_{A_I-A_{II}}$ between two rectangular plates with different values of a , b , and β with $h = 1.0$. (values in parentheses are $W_{A_I-A_{II}}$).

β	$a \backslash b$	0.4	1.0	4.0
$\pi/2$	0.4	(1.22)	(1.49)	(2.71)
		0.001	0.006	0.019
	1.0	(1.28)	(1.53)	(2.78)
		0.003	0.014	0.045
4.0	(1.40)	(1.72)	(3.17)	
	0.007	0.037	0.141	
$\pi/4$	0.4	(1.15)	(1.36)	(2.14)
		0.004	0.015	0.041
	1.0	(1.18)	(1.38)	(2.21)
		0.010	0.035	0.100
4.0	(1.30)	(1.53)	(2.52)	
	0.028	0.090	0.292	
0	0.4	(1.02)	(1.06)	(1.17)
		0.001	0.006	0.025
	1.0	(1.06)	(1.11)	(1.21)
		0.006	0.020	0.067
4.0	(1.17)	(1.21)	(1.36)	
	0.025	0.067	0.194	

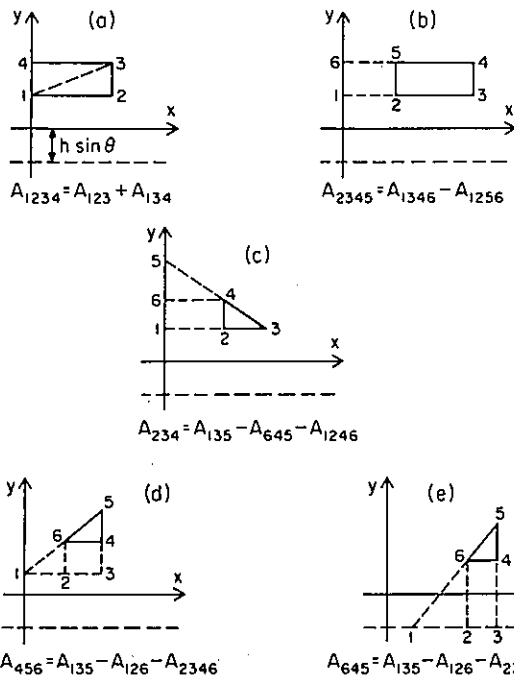


Fig. 3 Illustration on how an arbitrary right triangle can be constructed from fundamental right triangles

$$\int_{A_2} \nabla \times [f(r)\mathbf{r}_1 \times \mathbf{n}_1] \cdot \mathbf{n}_2 dA_2$$

$$= \int_{A_2} (\mathbf{n}_1 \cdot \mathbf{r}_1)(\mathbf{n}_2 \cdot \mathbf{r}_1) \left[f(r) - \frac{f(r)}{r} \right] dA_2$$

$$- \int_{A_2} (\mathbf{n}_1 \cdot \mathbf{n}_2) \left[f'(r) + \frac{f(r)}{r} \right] dA_2 \quad (A2)$$

The first term of the above equation can be simplified by Stoke's theorem. Equation (A2) thus becomes

$$\int_{A_2} (\mathbf{n}_1 \cdot \mathbf{r}_1)(\mathbf{n}_2 \cdot \mathbf{r}_1) \left[f'(r) - \frac{f(r)}{r} \right] dA_2$$

$$= \int_{S_2} [f(r)\mathbf{r}_1 \times \mathbf{n}_1] \cdot d\mathbf{S}_2 + \int_{A_2} (\mathbf{n}_1 \cdot \mathbf{n}_2) \left[f'(r) + \frac{f(r)}{r} \right] dA_2 \quad (A3)$$

where $d\mathbf{S}_2$ indicates a line integral around the boundary of A_2 . To yield the correct result, the line integral must be performed in a clockwise direction around A_2 when it is viewed from the origin. Because of the mathematical restriction on Stoke's theorem, it is important to note that equation (A3) is applied only when A_2 is a simply connected area (i.e., it has no "hole"). It is interesting to note that in the limit of

$$f(r) - \frac{f(r)}{r} = \frac{1}{r^2} \quad (A4)$$

equation (A3) is reduced to

$$\int_{A_2} \frac{(\mathbf{n}_1 \cdot \mathbf{r}_1)(\mathbf{n}_1 \cdot \mathbf{r}_1)}{r^2} dA_2 = -\frac{1}{2} \int_{A_2} \frac{(\mathbf{r}_1 \times \mathbf{n}_1)}{r} d\mathbf{S}_2 \quad (A5)$$

Equation (A4) is exactly the "contour-integral" expression for shape factor proposed originally by Moon [9] and Sparrow [10].

APPENDIX II

Since dA_1 cannot "see" any area with $y < -h \sin \theta$ or the plane $z = h$, it suffices to show that any area A_2 with $y \geq -h \sin \theta$ can be

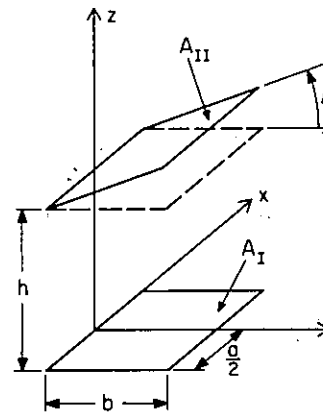


Fig. 4 Coordinate system used in the sample calculation

constructed from fundamental right triangles with orientations as shown in Fig. 2(b).

Figure 3(a) shows how an arbitrary rectangle with one edge lying on the y axis can be constructed as a sum of two fundamental right triangles. A rectangle situated away from the y axis can be generated as difference of these rectangles as shown in Fig. 3(b). Figure 3(c) shows how a "right oriented" right triangle can be constructed as a combination of rectangles and fundamental right triangles. Note that right triangles such as Δ_{135} can be constructed as a combination of a rectangle and the fourth fundamental right triangle. There are two possibilities for "left oriented" right triangles. They are demonstrated by Figs. 3(d) and 3(e).

Geometrically, it can be readily observed that any triangle on the plane $z = h$ with $y > -h \sin \theta$ can be constructed from right triangles oriented as shown in Figs. 3(c), 3(d) and 3(e). Since any polygon can by principle be expressed as a combination of a finite number of triangles, the fundamental solutions can thus serve as "building blocks" for solutions with A_2 being an arbitrary polygon. If A_2 has curve boundary, it can be approximately to any degree of accuracy by a finite number of a rectangle. The corresponding solution for the geometric transmittance and absorptance can therefore be approximated accurately as sum and difference of a finite number of fundamental solutions.

References

- Hottel, H. C., and Sarofim, A. F., *Radiation Transfer*, McGraw-Hill, New York, 1967.
- Siegel, R., and Howell, J. R., *Thermal Radiation Heat Transfer*, McGraw-Hill, New York, 1972.
- Oppenheim, A. K., and Bevans, J. T., "Geometric Factors for Radiative Heat Transfer Through an Absorbing Medium in Cartesian Co-ordinates," *ASME JOURNAL OF HEAT TRANSFER*, Nov. 1960, pp. 360-368.
- Dunkle, R. V., "Geometric Mean Beam Lengths for Radiant Heat-transfer Calculations," *ASME JOURNAL OF HEAT TRANSFER*, Vol. 86, No. 1, 1964, pp. 75-80.
- Tien, C. L., and Wang, L. S., "On the Calculation of Mean Beam Length to a Radiating Gas," *Journal of Quantitative Spectroscopy and Radiative Transfer*, Vol. 5, 1965, p. 465.
- Tien, C. L., and Ling, G. R., "On a Simple Correlation of Total Band Absorptance of Radiating Gases," *International Journal of Heat and Mass Transfer*, Vol. 12, 1969, pp. 1179-1181.
- Edwards, D. K., et al., "Radiation Heat Transfer in Nonisothermal Nongray Gases," *ASME JOURNAL OF HEAT TRANSFER*, Vol. 89, No. 3, 1967, pp. 219-229.
- Gradshteyn, I. S., and Ryzhik, I. M., *Table of Integrals, Series, and Products*, 4th ed., Academic Press, New York, 1965.
- Moon, P., *The Scientific Basis of Illuminating Engineering*, rev. ed., Dover Publication, New York, 1961.
- Sparrow, E. M., "A New and Simpler Formulation for Radiative Angle Factor," *ASME JOURNAL OF HEAT TRANSFER*, Vol. 85, No. 2, 1963, pp. 81-88.